2010

Microbial stimulation fully differentiates monocytes to DC-SIGN/ CD209 + dendritic cells for immune T cell areas

Cheolho Cheong

Ines Matos

Jae-hoon Choi

Cell

Microbial Stimulation Fully Differentiates Monocytes to DC-SIGN/CD209$^+$ Dendritic Cells for Immune T Cell Areas

Cheolho Cheong,[1,5,*] Ines Matos,[1,5] Jae-Hoon Choi,[1] Durga Bhavani Dandamudi,[1] Elina Shrestha,[1] M. Paula Longhi,[1] Kate L. Jeffrey,[2] Robert M. Anthony,[3] Courtney Kluger,[1] Godwin Nchinda,[1] Hyein Koh,[1] Anthony Rodriguez,[1] Juliana Idoyaga,[1] Maggi Pack,[1] Klara Velinzon,[4] Chae Gyu Park,[1,*] and Ralph M. Steinman[1,*]
[1]Laboratory of Cellular Physiology and Immunology and Chris Browne Center for Immunology and Immune Diseases
[2]Laboratory of Lymphocyte Signaling
[3]Laboratory of Molecular Genetics and Immunology
[4]Laboratory of Molecular Immunology, Howard Hughes Medical Institute
The Rockefeller University, 1230 York Avenue, New York, NY 10065, USA
[5]These authors contributed equally to this work
*Correspondence: ccheong@rockefeller.edu (C.C.), parkc@rockefeller.edu (C.G.P.), steinma@rockefeller.edu (R.M.S.)
DOI 10.1016/j.cell.2010.09.039

SUMMARY

Dendritic cells (DCs), critical antigen-presenting cells for immune control, normally derive from bone marrow precursors distinct from monocytes. It is not yet established if the large reservoir of monocytes can develop into cells with critical features of DCs in vivo. We now show that fully differentiated monocyte-derived DCs (Mo-DCs) develop in mice and DC-SIGN/CD209a marks the cells. Mo-DCs are recruited from blood monocytes into lymph nodes by lipopolysaccharide and live or dead gram-negative bacteria. Mobilization requires TLR4 and its CD14 coreceptor and Trif. When tested for antigen-presenting function, Mo-DCs are as active as classical DCs, including cross-presentation of proteins and live gram-negative bacteria on MHC I in vivo. Fully differentiated Mo-DCs acquire DC morphology and localize to T cell areas via L-selectin and CCR7. Thus the blood monocyte reservoir becomes the dominant presenting cell in response to select microbes, yielding DC-SIGN$^+$ cells with critical functions of DCs.

INTRODUCTION

Recent advances have clarified the origin of dendritic cells (DCs), a hematopoietic lineage specialized to present antigens and both initiate and control immunity (Heath and Carbone, 2009; Melief, 2008). In the bone marrow, a common monocyte-DC precursor (Fogg et al., 2006) gives rise to monocytes and other precursors termed common DC precursors (Naik et al., 2007; Onai et al., 2007) and pre-cDCs (Liu et al., 2009). The latter express intermediate levels of CD11c integrin and begin to synthesize MHC II products. Pre-cDCs move into the blood to seed both lymphoid and nonlymphoid tissues forming CD11c^{hi}, MHC II^{hi} DCs (Liu et al., 2009; Ginhoux et al., 2009). DCs in the steady state are dependent upon the hematopoietin, Flt3-L (D'Amico and Wu, 2003), whereas monocytes require macrophage colony-stimulating factor (M-CSF) (Geissmann et al., 2010). Flt3-L$^{-/-}$ mice have a severe deficit of DCs (Naik et al., 2007; Onai et al., 2007; Liu et al., 2009; Waskow et al., 2008), whereas monocytes are missing in mice lacking M-CSF receptor (c-fms or CD115) (Heard et al., 1987; Ginhoux et al., 2006). Thus, most DCs in the steady state are independent of monocytes.

Nevertheless, monocytes also can differentiate into DCs. Although first studied as macrophage precursors, mainly in vitro (de Villiers et al., 1994; Johnson et al., 1977), monocytes were later recognized to have an added potential to develop into DCs (monocyte-derived DCs [Mo-DCs]). This too has been studied primarily in cultures of human blood monocytes (Romani et al., 1994; Sallusto and Lanzavecchia, 1994). Monocytes, upon culture for several days in GM-CSF and IL-4, acquire a typical probing or dendritic morphology, lose the capacity to phagocytose, and adhere to various tissue culture surfaces but acquire strong capacities to initiate immunity. Mo-DCs can immunize humans (Dhodapkar et al., 1999; Schuler-Thurner et al., 2000) and home to the T cell areas of lymph nodes (LNs) (De Vries et al., 2003). Monocytes are ~20 times more abundant than DCs in blood and marrow, so the mobilization of this monocyte reservoir in vivo to generate potent antigen-presenting DCs needs to be elucidated.

Several reports have begun to document in mice the differentiation of CD11c$^-$ and MHC II$^-$ blood monocytes into large numbers of CD11c$^+$ MHC II$^+$ Mo-DCs during different models, e.g., *Leishmania major* infection via the skin (Leon et al., 2007), intravenous infection with *Listeria monocytogenes* (Serbina et al., 2003), influenza virus infection via the airway (Nakano et al., 2009), *Aspergillus fumigatus* in the lung (Hohl et al., 2009), T cell-mediated colitis (Siddiqui et al., 2010), and injection

of the adjuvant, alum (Kool et al., 2008). These Mo-DCs presented protein antigens to TCR transgenic $CD4^+$ T cells and are distinguished from classical DCs by expression of the Gr-1/Ly6C monocyte markers. However, many classical functional features of DCs have not been assessed, including a peculiar probing morphology, localization to T cell areas of lymphoid organs in a position to find and activate rare clones of specific T cells, and efficient antigen capture and processing.

The latter includes the capacity for cross-presentation. This is the processing of captured proteins onto MHC I without the need for synthesis in antigen-presenting cells (APCs) (Heath and Carbone, 2001). Through cross-presentation to $CD8^+$ T cells, DCs present nonreplicating antigens, e.g., from dying cells (Liu et al., 2002; Luckashenak et al., 2008), noninfectious microbes (Moron et al., 2003), and immune complexes (Regnault et al., 1999). The $CD8^+$ subset of classical DCs are specialized for cross-presentation (den Haan et al., 2000; Schnorrer et al., 2006; Dudziak et al., 2007; Sancho et al., 2009), but Mo-DCs have not been assessed in vivo.

To address these gaps, markers are required to identify Mo-DCs. Here we describe a unique approach using recently isolated monoclonal anti-DC-SIGN/CD209a antibodies (Cheong et al., 2010). We had previously defined in mice the DC-SIGN or CD209a gene syntenic with human DC-SIGN/CD209 (Park et al., 2001). DC-SIGN is a hallmark of human Mo-DCs in culture (Geijtenbeek et al., 2000b) but is not detected on the rich network of presumably monocyte-independent DCs in human LNs in the steady state (Granelli-Piperno et al., 2005). We now find that anti-mouse DC-SIGN/CD209a monoclonal antibodies (mAbs) distinguish Mo-DCs from classical DCs in cell suspensions and tissue sections. We will report that the full differentiation of monocytes to DC-SIGN/$CD209a^+$ Mo-DCs does occur in vivo and can be initiated by lipopolysaccharide (LPS) or LPS-expressing bacteria. In contrast to prior reports on inflammatory monocytes, these Mo-DCs rapidly lose expression of monocyte markers Gr-1/Ly6C and CD115/c-fms, markedly upregulate expression of TLR4 and CD14, acquire the probing morphology of DCs, localize to the T cell areas, and through Trif signaling become powerful antigen-capturing and -presenting cells, including cross-presentation of gram-negative bacteria.

RESULTS

DC-SIGN/CD209a Marks Mouse Mo-DCs with Strong Antigen-Presenting Activity

To determine if new mAbs to mouse DC-SIGN/CD209a can identify Mo-DCs, as occurs with cultured human Mo-DCs (Geijtenbeek et al., 2000b), we cultured bone marrow monocytes (SSC^{lo} cells with high Ly6C and CD11b; Figure S1A available online; Naik et al., 2006) with two cytokines, GM-CSF and IL-4, as described for blood monocytes (Schreurs et al., 1999). After 4–7 days, we recovered ~80% of the plated cells. Most had converted to large nonadherent cells that extended and retracted sheet-like processes in several directions from the cell body (Figure 1A, left), which is the hallmark, probing morphology of DCs (Steinman and Cohn, 1973; Lindquist et al., 2004). A polyclonal Ab to mouse DC-SIGN detected low levels of the 30 kDa protein in fresh monocytes, but within 2 days of culture, DC-SIGN and MHC II were upregulated markedly (Figure 1A, right), particularly with IL-4 and GM-CSF in combination, whereas no DC-SIGN was expressed by marrow granulocytes similarly cultured (Figure S1B).

To establish differentiation to DCs, we confirmed that fresh marrow and blood monocytes did not react with mAbs to DC-SIGN, MHC II, or CD11c (Figure S1B), but when cultured in GM-CSF and IL-4, strong reactivity developed (Figure 1B, top). The combination of GM-CSF and IL-4, but not single cytokines or other hematopoietins like Flt3-L and M-CSF, allowed monocytes to express MHC II and CD11c and develop a DC morphology. When we compared marrow monocytes before and after culture in GM-CSF and IL-4 (Figure 1C, left, days 0 and 4) to spleen monocytes and classical DCs (Figure 1C, right panels), we found that Mo-DCs like spleen DCs lacked M-CSF receptor or CD115, a key receptor for monocyte development, whereas both marrow and splenic monocytes expressed CD115 (Figure 1C). Splenic but not Mo-DCs expressed Flt3 or CD135 (Figure 1C), the receptor for Flt3-L, a major hematopoietin for DCs derived from nonmonocytic precursors.

During differentiation, Mo-DCs also lost the Gr-1 and Ly6C markers of monocytes and reduced their levels of F4/80 but retained high expression of CD11b and CD172a found on both monocytes and DEC-205^- $CD8^-$ monocyte-independent, spleen DCs (Figure 1C). Monocytes and Mo-DCs lacked $CD8\alpha\alpha$, expressed by the DEC-205^+ $CD8^+$ subset of splenic DCs, but Mo-DCs expressed high levels of CD24, like DEC-205^+ $CD8^+$ splenic DCs (not shown). The data in Figures 1B and 1C indicate that monocytes acquire many surface features of splenic DCs except that Mo-DCs express DC-SIGN and lack Flt3 or CD135.

To test if DC-$SIGN^+$ Mo-DCs shared functions with splenic DCs, we used the mixed leukocyte reaction (MLR), an example of the immune-initiating function of DCs (Steinman and Witmer, 1978). In these and all T cell studies, we used CSFE-labeled T cells and monitored the expansion of dividing or $CFSE^{lo}$ cells, as in Figures S1C and S1D. Mo-DCs induced with GM-CSF and IL-4 stimulated a strong MLR, whereas monocytes cultured under other conditions were weak (GM-CSF) or inactive (IL-4, M-CSF, Flt3-L) (Figure S1C).

To evaluate presentation of protein antigens, we used TCR transgenic T cells as responders and compared Mo-DCs to two subsets of classical splenic DCs (DEC-205^+ and DEC-205^-, corresponding to $CD8^+$ and $CD8^-$ DCs). We used 40 μg/ml, a limiting concentration malarial circumsporozoite protein (CSP, expressed in bacteria), and Ovalbumin (OVA). The Mo-DCs were superior APCs when using graded doses of each type of DC (Figure 1D, green).

To compare Mo-DCs with classical DCs that had also been derived from marrow cultures, we used a Flt3-L culture system as described by Naik et al. (2005) (Figure S1E). Over a range of protein concentrations and cell doses, Mo-DCs were superior cross-presenting cells relative to Flt3-L expanded, $CD8^+$, and $CD8^-$ DC equivalents (Figure S1F). The Mo-DCs also were superior to $CD8^+$ DCs when irradiated, stably expressing OVA-CHO cells were used as the antigen (Figure 1E). Thus in vitro derived Mo-DCs are marked by DC-SIGN and are functionally strong APCs, including cross-presentation.

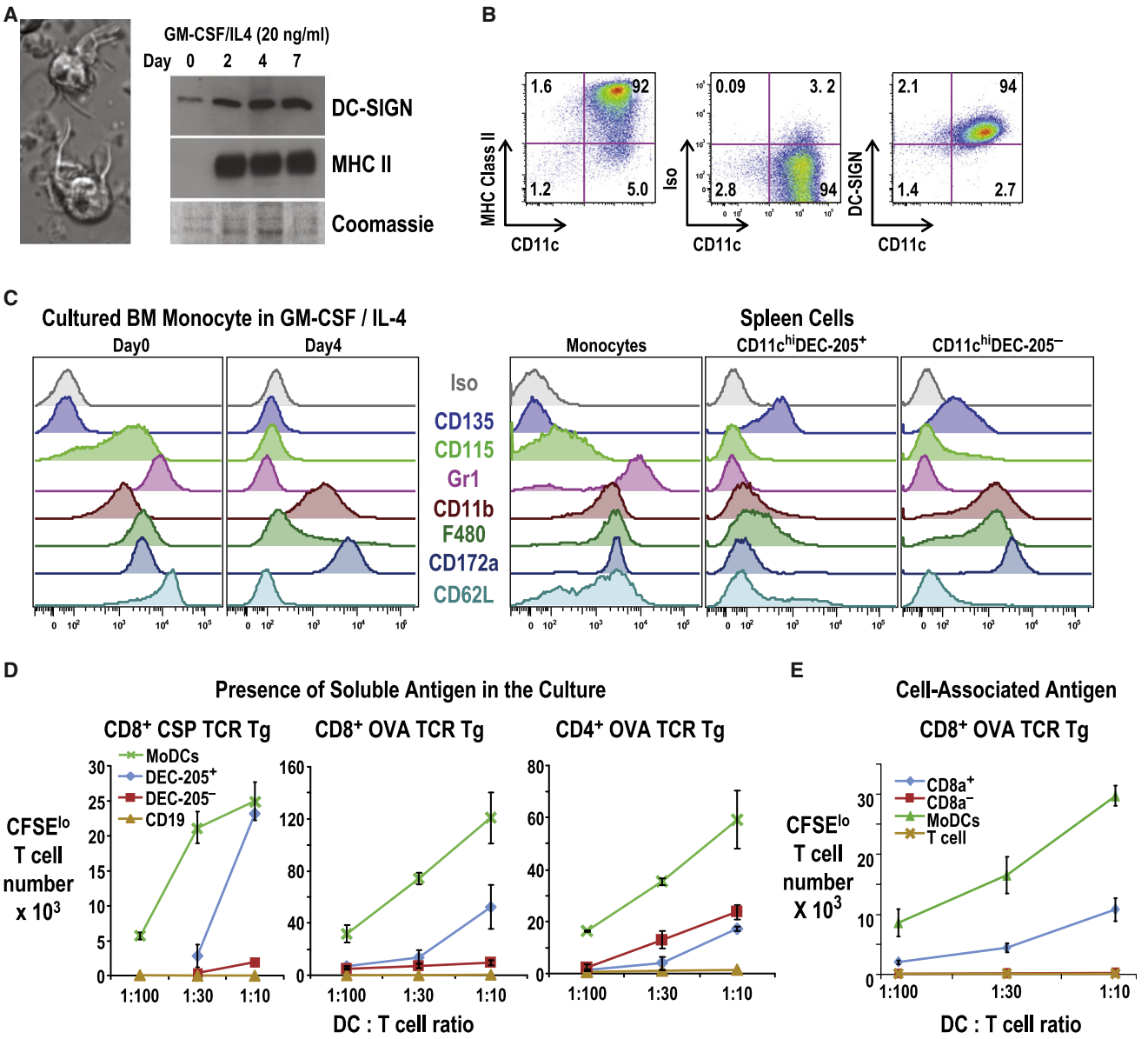

Figure 1. DCs Derived from Marrow Monocytes Express DC-SIGN and Are Potent APCs

(A) Marrow monocytes (Figure S1) were cultured in GM-CSF and IL-4 for 4–7 days. (Left) DIC image with typical dendritic morphology. (Right) Western blot with rabbit polyclonal αDC-SIGN and mAb KL295 αMHC II.

(B) As in (A), showing MHC II, CD11c, and DC-SIGN Alexa 647-MMD3 (or isotype control, middle panel) on Mo-DCs.

(C) Surface markers on freshly isolated monocytes, GM-CSF/IL-4-induced Mo-DCs, and fresh spleen populations.

(D) Presentation of CSP or OVA, 40 μg/ml, to TCR transgenic T cells by graded doses of Mo-DCs or CD11c^{hi} DEC-205^{+} and DEC-205^{-} DCs from spleen. Gating strategy for CFSE^{lo} T cells is in Figure S1D.

(E) Presentation of stably transduced, irradiated CHO-OVA cells by graded doses of different populations of DCs cultured from bone marrow (DC:T cell ratio on the x axis), including the equivalents of CD8^{+} and CD8^{-} classical DCs from Flt3-L expanded marrow cultures (Figure S1E). Representative of 2–3 experiments in triplicate or quadruplicate cultures.

Error bars = standard deviation (SD) (D and E).

TLR4 Agonists Rapidly Recruit DC-SIGN^{+} Cells to the T Cell Area of Lymph Nodes

To find out if comparable Mo-DCs develop in vivo in response to microbial stimuli, we treated mice intravenously (i.v.) with agonists for individual Toll-like receptors (TLRs) and looked for DC-SIGN/CD209a^{+} cells in LNs 12–24 hr later. We also assessed mannose receptor/CD206 because both CD206 (Sallusto et al., 1995) and DC-SIGN/CD209 (Geijtenbeek et al., 2000b) are induced when cultured human monocytes become Mo-DCs. Using LPS, we observed a 10-fold increase in

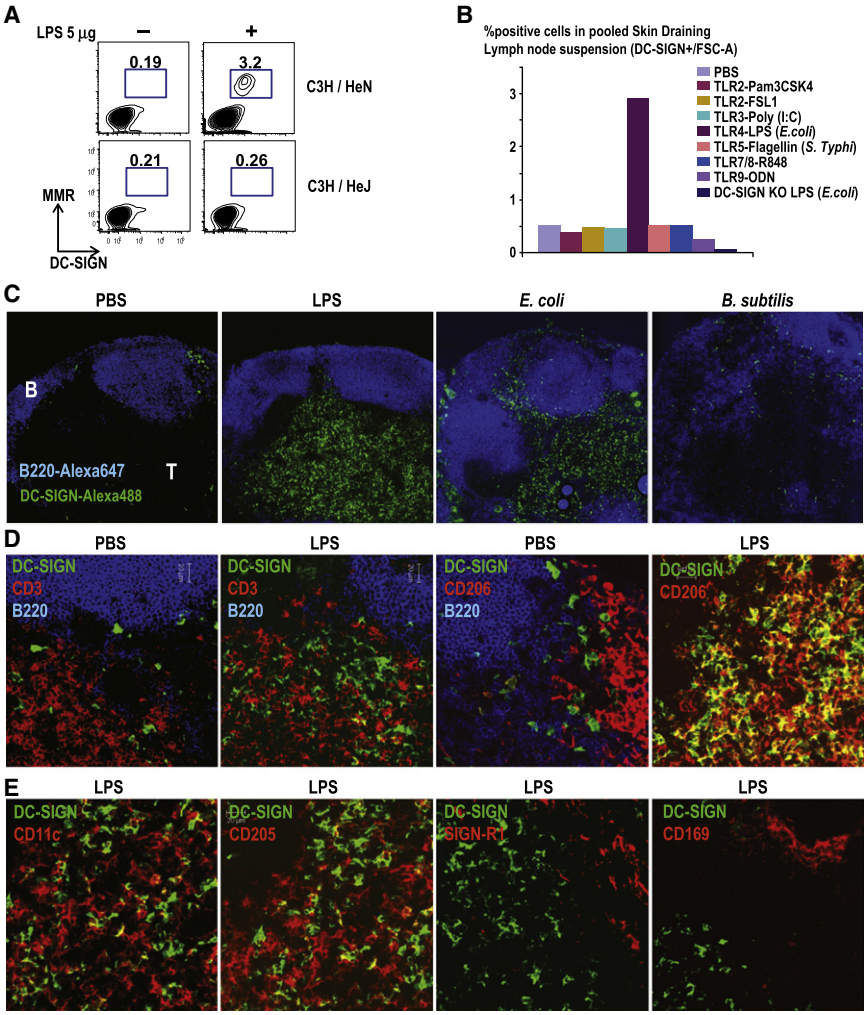

Figure 2. Mobilization of DC-SIGN$^+$ Mo-DCs to the T Cell Areas of Lymph Nodes

(A) TLR4-competent (C3H/HeN) or TLR4 mutant (C3H/HeJ) mice were injected with 5 μg of LPS i.v. After 24 hr, lymph node cells were stained intracellularly with Alexa 647 MMD3 α-DC-SIGN and Alexa 488 α-MMR/CD206 mAbs.

(B) Mice were injected i.v. with 10 μg of α-DC-SIGN-Alexa 647 mAb and 5 μg of TLR agonist.

(C) Labeling of frozen sections with the indicated mAb 12–24 hr after PBS, 5 μg LPS i.v., or 5 × 10^6 heat-killed *E. coli* or *B. subtilis* i.v. Alexa 647 B220 mAb marks B cell areas (blue). 100× magnification.

(D and E) Lymph node sections from PBS- or LPS-treated mice were stained with the indicated mAb. 400× magnification.

DC-SIGN/CD209a$^+$ CD206$^+$ cells in skin-draining nodes 12–24 hr later (Figure 2A) but not in spleen or mesenteric nodes (not shown). Expansion took place in C3H/HeN but not C3H/HeJ TLR4 mutant mice, indicating a need for TLR4 (Figure 2A, compare top and bottom right). However, DC-SIGN/CD209a$^+$ cells did not expand to other TLR agonists like Pam3CSK4, poly(I:C), Flagellin, R848, and CpG, for TLR2, 3, 5, 7/8, and 9, respectively (Figure 2B).

To determine whether Mo-DCs localize to T cell areas like authentic DCs, we used new anti-DC-SIGN mAbs (Cheong et al., 2010) to label lymph node sections. In PBS mice, there were relatively few DC-SIGN$^+$ cells, mainly in interfollicular regions, beneath SIGN-R1/CD209b$^+$ subcapsular macrophages and between B220$^+$ B cell follicles (Figure 2C, left and Figure S2A). However, 12 hr after LPS i.v., DC-SIGN$^+$ cells were abundant and localized to T cell areas, regions in which DCs have been shown to present antigens to recirculating antigen-specific T cells (Stoll et al., 2002; Mempel et al., 2004; Miller et al., 2004; Shakhar et al., 2005) (Figure 2C). Likewise, DC-SIGN$^+$ cells accumulated in the T cell areas when we injected LPS-bearing, heat-killed *E. coli* i.v. and subcutaneously (s.c.) but not LPS-lacking *B. subtilis* by these routes (Figure 2C) or *Listeria monocytogenes* s.c. (not shown).

To determine if DC-SIGN$^+$ cells were distinct from DCs and macrophages in the lymph node, we double-labeled for DC-SIGN and several markers. In PBS-injected mice, the few DC-SIGN$^+$ cells were distinct from macrophages in subcapsular and medullary regions of lymph node, which in steady state express CD206 (Figure 2D) and SIGN-R1/CD209b (Figure S2). However, in LPS-injected mice, there was a major expansion of cells in the T cell area expressing both CD206 and DC-SIGN/CD209a (Figure 2D and Figure S2). The DC-SIGN$^+$ cells mobilized to the T cell areas by LPS were clearly distinct from other DCs, which expressed higher levels of CD11c, as well as DEC-205/CD205 and Langerin/CD207 (Figure 2E and Figure S2). Also, DC-SIGN$^+$ cells did not colabel with markers that are abundant on lymph node macrophages, such as SIGN-R1/CD209b and CD169 (Figure 2E, right panels and Figure S2) and F4/80 (not shown). DC-SIGN/CD209a$^+$ Mo-DCs also lacked CD115 and Ly6C found on monocytes and inflammatory monocytes (Geissmann et al., 2003) (not shown). Therefore, DC-SIGN marks abundant cells in the T cell areas from LPS-treated mice, which express molecules distinct from classical DCs, macrophages, and monocytes.

Mo-DCs Can Be Selectively Labeled with Injected Anti-DC-SIGN/CD209a Antibody and Isolated from Classical DCs in Lymph Nodes

To compare the properties of LPS-mobilized DC-SIGN$^+$ cells to other DCs in LNs, we needed a strategy to separate the cell types. However, the problem we faced was that most DC-SIGN is inside the cell and not on the cell surface, preventing the separation of cell-surface-labeled DC-SIGN$^+$ cells. To

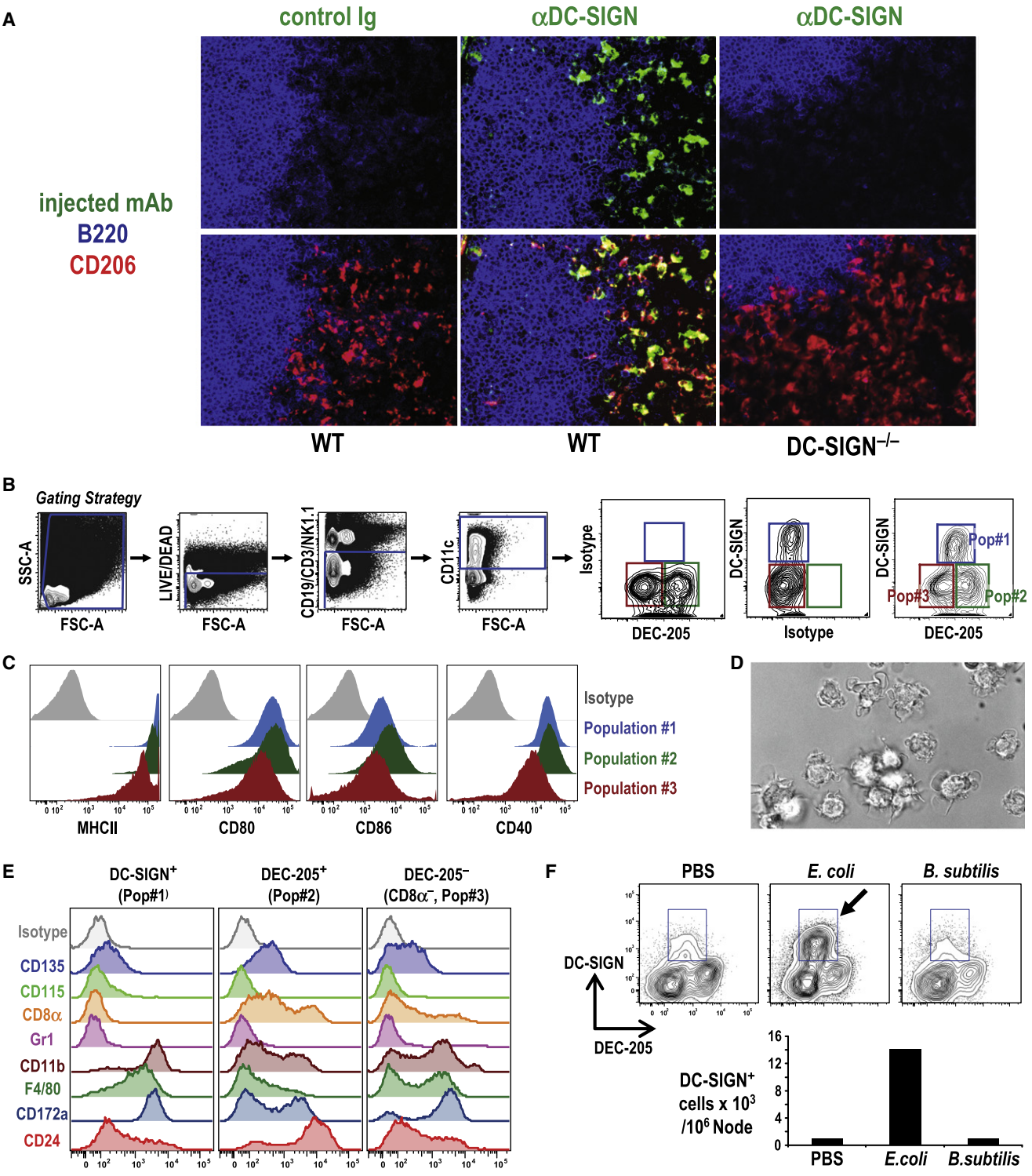

Figure 3. DC-SIGN$^+$ Mo-DCs Are Induced upon Treatment with LPS or LPS-Bacteria

(A) Thirty micrograms Alexa 488 MMD3 α-DC-SIGN or control mAb were injected i.v. with LPS into WT or DC-SIGN$^{-/-}$ mice. Twelve hours later, lymph node sections were fixed and stained with rabbit α-Alexa 488 to visualize the injected mAb in green. α-MMR/CD206 (red) identifies Mo-DCs, and A647 B220 mAb (blue) B cells. 400× magnification.

(B) Separation of three lymph node DC populations 12 hr after injecting i.v. 10 μg of Alexa 647 MMD3 α-DC-SIGN mAb plus 5 μg of LPS. Skin-draining lymph node cells were stained for lymphocyte lineage markers (CD3, CD19, NK1-1 [or DX-5]), CD11c, and DEC-205. Live, lineage$^-$ CD11c$^+$ cells were gated and three populations defined (Pop#1, #2, #3). Isotypes for DC-SIGN and DEC-205 are mouse IgG2c and rat IgG2a, respectively.

overcome this obstacle, during injection of LPS (or PBS controls), we also included 10 μg of Alexa dye-labeled MMD3 anti-DC-SIGN mAb, or isotype-matched control mAb, to allow the DC-SIGN$^+$ cells to take up the fluorescent mAb. When we examined sections of the injected LNs (Figure 3A), we found that the injected anti-DC-SIGN mAb labeled abundant dendritic profiles in the T cell area, but only if the mice had received LPS. No such profiles were seen if we injected isotype control mAb, or if we injected Alexa 488-labeled MMD3 into DC-SIGN$^{-/-}$ mice (Figure 3A), which did mobilize numerous macrophage mannose receptor (MMR)/CD206$^+$ cells in response to LPS (Figure 3A and Figure S2E). The anti-DC-SIGN mAb-targeted cells did not express detectable CD115, but this M-CSF receptor strongly marked lymph node medullary macrophages, and had low levels of CD11c but no DEC-205, which were expressed by classical DCs in the lymph node (not shown).

Therefore to isolate Mo-DCs, we injected LPS together with labeled MMD3 mAb (or isotype control mAb) and made cell suspensions. To identify DCs, we gated on lymphocyte lineage-negative, CD11c$^+$ cells, and we surface labeled for DEC-205 on cross-presenting classical DCs. In LNs from mice injected with LPS plus-labeled MMD3 mAb, there was a specifically stained DC-SIGN$^+$ population, as there was no staining if isotype control mAb was injected (Figure 3B), or if we studied DC-SIGN$^{-/-}$ mice (Figure S3A). Labeling with MMD3 was comparable in wild-type (WT) and Fc receptor $\gamma^{-/-}$ mice, further indicating that labeling required DC-SIGN and was not Fc mediated (Figure S3B). The CD11c$^+$ lymphocyte-negative cells also had DEC-205$^+$ and DEC-205$^-$ populations, both lacking DC-SIGN. Thus LNs from LPS-treated mice have three populations: population #1 corresponds to DC-SIGN/CD209a$^+$ DCs, which we will show derive from monocytes, whereas populations #2 and #3 correspond to DEC-205$^+$ (including CD8$^+$, Figure S3A) and DEC-205$^-$ resident DCs (Vremec and Shortman, 1997) (Figure 3B and Figures S3A and S3B).

When tested for surface markers following cell sorting, all three populations of DCs from LPS-treated LNs expressed high levels of MHC II, which is expected of DCs, and all expressed CD40, 80, and 86 with the DC-SIGN$^+$ and DEC-205$^+$ subsets having the highest levels (Figure 3C). However, the DC-SIGN$^+$ population had lower levels of CD11c (not shown). We also verified that the sorted DC-SIGN$^+$ cells had the probing morphology of DCs (Figure 3D and Movie S1 for video). All three DC populations likewise failed to stain for CD115/c-fms, but DC-SIGN$^+$ cells lacked CD135/Flt3, which was expressed by lymph node resident DCs (Figure 3E). Like DEC-205$^-$ classical DCs, DC-SIGN$^+$ DCs were CD11b$^+$ and CD172a/SIRPα^{hi}, F4/80$^+$, CD24^{lo}, and CD8$^-$ (Figure 3E).

To test LPS-bearing bacteria, we injected the labeled MMD3 mAb together with either dead or live *E. coli* and, 12 hr later, stained cells from draining LNs. Either dead or live *E. coli*, but not dead or live *B. subtilis* that lacked LPS, mobilized DC-SIGN$^+$ cells and upregulated CD86 on splenic DCs if injected i.v. (Figure 3F and Figure S3C). These data indicate that cells with the morphology and markers of Mo-DCs accumulate in vivo in response to LPS and LPS$^+$ bacteria, and they resemble CD8$^-$ DEC-205$^-$ resident DCs except for selective DC-SIGN/CD209a and MMR/CD206 expression, two uptake receptors abundant on human Mo-DCs ex vivo (Sallusto et al., 1995; Granelli-Piperno et al., 2005).

DC-SIGN$^+$ MMR$^+$ Mo-DCs in LPS-Stimulated Lymph Nodes Derive from Monocytes

To determine whether LPS mobilized DC-SIGN$^+$ cells from monocytes, we injected 2 × 10^6 marrow monocytes from CD45.2$^+$ mice i.v. into CD45.1$^+$ hosts. Next day, the mice were injected i.v. with labeled MMD3 mAb and 5 μg of LPS. Twenty-four hours later, skin-draining LNs were tested by flow cytometry for Mo-DC recruitment. In three experiments, with three mice each, LPS induced an increase in CD45.2$^+$ donor-derived, DC-SIGN/CD209a$^+$ and MMR/CD206$^+$ cells in all mice, whereas donor-derived cells were absent in nodes of PBS-injected mice (Figure 4A).

To establish the monocyte origin of LPS-recruited Mo-DCs by an alternative method, we focused on LysMcre × iDTR mice, in which treatment with diphtheria toxin (DT) depletes monocytes and macrophages (Goren et al., 2009). We confirmed that a single dose of DT i.v. decreased >80% of blood monocytes 12 hr later (Figure 4B). DT-treated, LPS-injected WT mice generated CD11c$^+$ DC-SIGN$^+$ cells normally (Figure 4B, right, arrow), but DT-treated, LPS-injected LysMcre × iDTR mice failed to generate Mo-DCs, although the classical monocyte-independent DC subsets were normally represented (Figure 4B, right). Likewise in tissue sections, DC-SIGN$^+$ DCs were not recruited into the T cell areas of LNs of LPS-treated LysMcre × iDTR mice upon DT treatment, but DEC-205$^+$ DCs were abundant in LPS- and DT-treated WT and LysMcre × iDTR mice (Figure 4C, green versus red), again showing that Mo-DCs derived from monocytes, whereas classical DCs did not.

To test whether the spleen was needed, a recently recognized source of monocytes (Swirski et al., 2009), we studied splenectomized mice. However after LPS injection, these mice normally mobilized DC-SIGN/CD209a$^+$ MMR/CD206$^+$ Mo-DCs (Figure S4A).

To selectively deplete classical DCs, we employed Flt3$^{-/-}$ mice, which lack classical DCs because of a need for Flt3 signaling. We confirmed a loss of classical DCs in Flt3$^{-/-}$ mice (Waskow et al., 2008), but in contrast, LPS comparably mobilized Mo-DCs from Flt3$^{-/-}$ and WT mice using either DC-SIGN/CD209a or MMR/CD206 as markers (Figure 4D and Figure S4B). To determine whether cell proliferation was involved, we labeled mice with BrdU during the 12 hr treatment with LPS, but no labeling was evident in contrast to the basal level of BrdU labeling of classical DCs (Figure S4C). These results provide considerable evidence for the monocyte origin of DC-SIGN$^+$ DCs in LNs from LPS-treated mice.

(C) Expression of maturation markers on three DC populations.
(D) Representative morphology (DIC images) of DC-SIGN$^+$ cells sorted from LNs of LPS-treated mice as in (B). 600× magnification.
(E) Three DC populations as in (B) were sorted and stained with PE-mAbs.
(F) As in (B), but fluorescence-activated cell sorting (FACS) analyses and total numbers of lineage$^-$ CD11c$^+$ cells from mice 12 hr after i.v. injection of MMD3 α-DC-SIGN mAb plus killed *E. coli* or *B. subtilis* (data with live organisms are in Figure S3C).

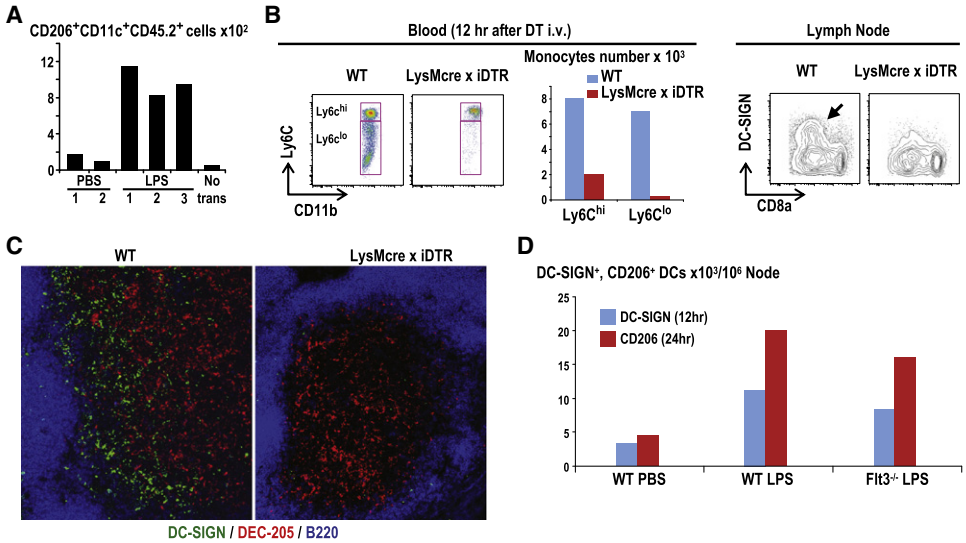

Figure 4. Monocyte Origin of DC-SIGN$^+$ Mo-DCs

(A) CD45.2$^+$ marrow monocytes were transferred i.v. into CD45.1$^+$ hosts. Twenty-four hours later, PBS or 5 μg of LPS was injected i.v. with 10 μg Alexa 647-MMD3 α-DC-SIGN, and 24 hr later, DC-SIGN$^+$ CD206$^+$ DCs of CD45.2 origin were enumerated. This is one of three similar experiments.

(B) WT and LysMCre × iDTR mice were injected with DT, and 12 hr later, blood monocytes (Ly6G$^-$ CD115$^+$ CD11b$^+$ Ly6C$^{hi/lo}$) were analyzed (left panels). Twenty-four hours after DT, 5 μg of LPS plus 10 μg of MMD3-Alexa 647 mAb were given i.v., and 12 hr later, skin-draining lymph node cells were analyzed as CD19/CD3/NK1.1$^-$ and CD11c ^{high} and segregated into three DC populations (right) to look for DC-SIGN$^+$ Mo-DCs (arrow).

(C) Lymph node sections were stained for Mo-DCs with α-DC-SIGN (BMD10, green), resident DCs with α-DEC-205 (NLDC145, red), and B cells with α-B220 (blue) at 100× magnification.

(D) WT and Flt3$^{-/-}$ mice were injected with 5 μg of LPS and 10 μg of MMD3-Alexa 647 α-DC SIGN mAb to enumerate Mo-DCs expressing DC-SIGN (blue) or MMR/CD206 (red) 24 hr later. Shown are cells/10^6 lymph node cells from two independent experiments with 2 mice/group.

L-Selectin and CCR7 Are Required for LPS to Generate Mo-DCs

To begin to identify mechanisms of Mo-DC mobilization, we evaluated the lymph node homing molecule used by lymphocytes, L-selectin/CD62L, which is also expressed on monocytes prior to their becoming Mo-DCs (e.g., in Figure 1C). We treated mice with isotype control or anti-CD62L (MEL-14) mAb and 1 hr later injected LPS. Anti-CD62L blocked Mo-DC formation in LNs using immunolabeling of sections and cell suspensions (Figures 5A and 5B).

To identify the required chemokine receptors, we tested four chemokine receptor knockout mice. Accumulation of DC-SIGN$^+$ Mo-DCs was critically dependent on CCR7 (Figure 5C, right). Only a partial but statistically significant decrease in Mo-DCs was noted in CCR2$^{-/-}$ mice (Figure S5A), whereas CCR5 and CCR6 were not necessary (Figure 5C). Monocytes disappeared normally from the blood in LPS-treated CCR7$^{-/-}$ mice, and CCR7 was not required to generate Mo-DCs in vitro (Figures S5B and S5C). In all these experiments, we verified that spleen DCs in the knockout mice responded normally to LPS by upregulating CD86 (Figure 5C, right). To establish that the need for CCR7 was cell intrinsic, we made mixed bone marrow chimeras with 50:50 mixes of WT and CCR7$^{-/-}$ donor cells, each marked with CD45.1 and CD45.2 and injected into CD45.1$^+$ WT hosts. Six weeks later, we certified chimerism in the blood (Figure 5D, left) and injected LPS to recruit DC-SIGN/CD209a$^+$ MMR/CD206$^+$ DCs. LPS greatly reduced the number of monocytes in the blood (Figure 5D, middle), but only CD45.1$^+$ WT cells and not CD45.2$^+$ CCR7$^{-/-}$ cells formed Mo-DCs (Figure 5D, right), indicating that the need for CCR7 by Mo-DCs is cell intrinsic.

Mo-DCs Efficiently Present Proteins and Bacteria Captured In Vivo to T Cells

To test the antigen-presenting functions of Mo-DCs, we initially sorted three populations of CD11c^{hi} DCs from inflamed LNs using CD11c, DEC-205, and DC-SIGN as markers as in Figure 3B. All three DC types from LPS-treated mice effectively stimulated allogeneic T cells in the MLR assay, with Mo-DCs being moderately more active (Figure 6A, left and Figure S6). Surprisingly, Mo-DCs were comparable or superior to classical DCs in presenting two different proteins (OVA, which is glycosylated, and CSP, which is nonglycosylated) to CD8$^+$ and CD4$^+$ TCR transgenic T cells (Figure 6A). Thus just like the Mo-DCs that can be generated in culture by adding GM-CSF and IL-4 to monocytes, LPS-mobilized Mo-DCs in vivo are as good or better presenting cells than classical DCs, including cross-presentation.

To consider antigen capture in vivo, we injected LPS, then soluble CSP or OVA protein s.c. 10 hr later. At 12 hr, or 2 hr after CSP/OVA injection, we isolated DC-SIGN$^+$ Mo-DCs as well as DEC-205$^+$ and DEC-205$^-$, DC-SIGN$^-$ classical DCs from the nodes. When added in graded doses to TCR transgenic, CD4$^+$ and CD8$^+$ T cells without further antigen, Mo-DCs were again comparable or superior to classical DCs for both CSP and OVA (Figure 6B and Figure S6), showing that these cells capture and present on both MHC I and II in vivo.

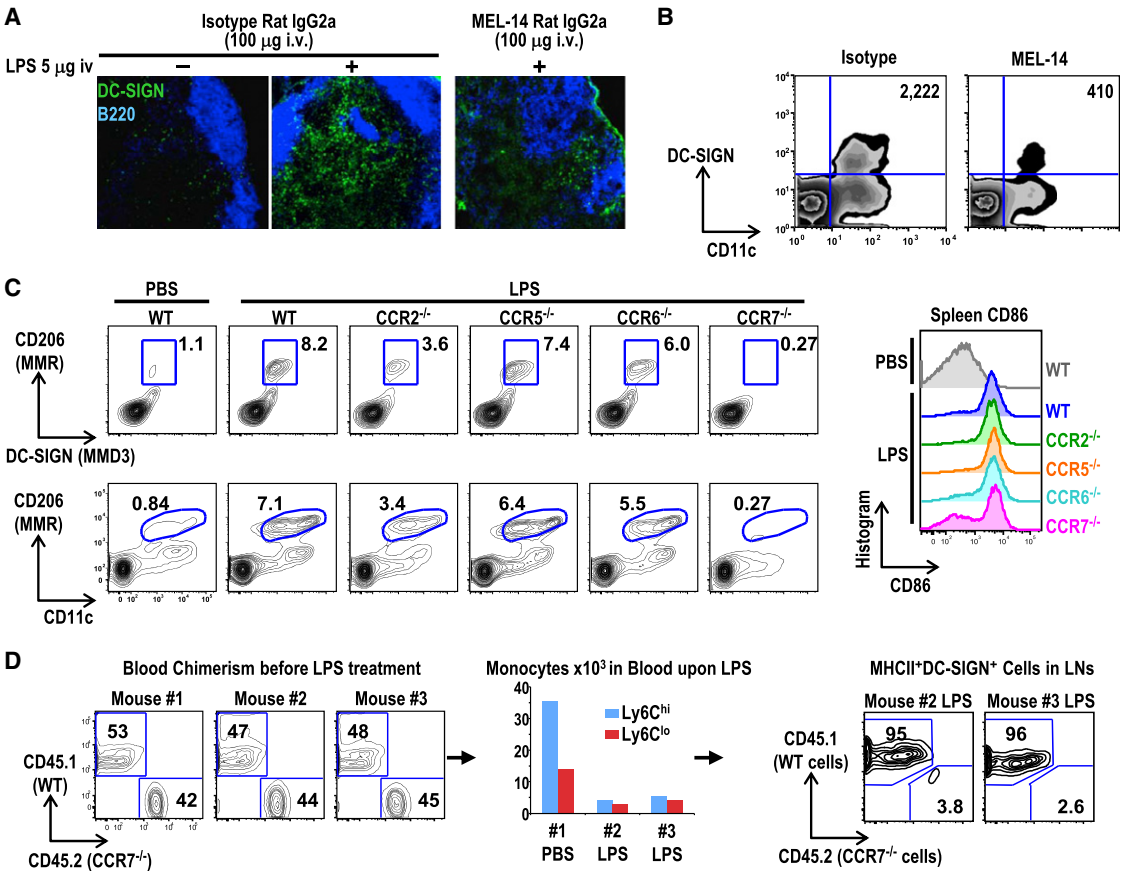

Figure 5. L-Selectin and CCR7-Dependent Trafficking of DC-SIGN$^+$ Mo-DCs

(A and B) mAb to block L-selectin (MEL-14, 100 μg i.v.) was given 1 hr before injection of LPS and α-DC-SIGN mAb. After 24 hr, LNs were analyzed by staining at 100× magnification (A) or FACS (B).

(C) Chemokine receptor KO mice were injected with LPS i.v., and 24 hr later, lymph node cells were stained for intracellular DC-SIGN and MMR/CD206. Systemic injection of LPS was confirmed by CD86 upregulation on spleen DCs (right).

(D) Blood chimerism 6 weeks after lethal irradiation and reconstitution with CD45.1 (WT) and CD45.2 (CCR7$^{-/-}$) in CD45.1 hosts (left). Twelve hours after LPS, blood monocytes had largely disappeared (middle). LNs from these same animals were stained for CD45.1, CD45.2, DC-SIGN, and MHC II to show that Mo-DCs were WT in origin.

To determine the type of T cell that was developing in response to antigen-presenting Mo-DCs, we collected the medium from 4 day cocultures of OT-II CD4$^+$ TCR transgenic T cells with Mo-DCs that had captured OVA in vivo. The Mo-DCs induced strong production of IFN-γ and IL-2 but not IL-4, IL-10, or IL-17 (Figure 6C), suggesting Th1 differentiation.

To evaluate presentation of bacterial antigens, we injected recombinant *E. coli* OVA (or *E. coli* control). Twelve hours later, we isolated three populations of DCs from the LNs. Mo-DCs were even more effective than DEC-205$^+$ classical cross-presenting DCs, whereas DEC-205$^-$ DCs did not cross-present bacteria (Figure 6D).

Mo-DCs Selectively Express CD14, a Needed Coreceptor for Trif-Dependent LPS Signaling

To begin to understand why LPS and gram-negative bacteria were superior agonists for mobilizing Mo-DCs, we first used quantitative PCR to assess expression of several TLRs in marrow monocytes and Mo-DCs. Both cells expressed several TLRs, but TLR4 and its coreceptor CD14 were markedly upregulated in Mo-DCs (Figure 7A).

To pursue the contribution of the LPS coreceptor, CD14, we used monoclonal anti-CD14 to show that monocytes were selectively CD14$^+$ in blood (Figure S7A), whereas among CD11c^{hi} DCs in the LNs from LPS-stimulated mice, only DC-SIGN$^+$ Mo-DCs were CD14$^+$ (Figure 7B). When we studied CD14$^{-/-}$ mice, which lacked CD14 on monocytes (Figure S7B), LPS injection failed to mobilize Mo-DCs (Figure 7C). We then compared mice lacking the MyD88 and Trif adaptors for TLR4 signaling, where CD14 is a known coreceptor for MyD88-independent, Trif-dependent signaling (Jiang et al., 2005). Trif, not MyD88, was essential for LPS to mobilize Mo-DCs (Figure 7D) and to upregulate CD86 on splenic DCs (Figure S7C). CD14$^+$ DCs accumulated with identical kinetics to DC-SIGN$^+$ Mo-DCs, peaking at 24 hr and becoming the dominant DCs in LNs (Figure 7E and Figure S7D). Together, the data indicate that CD14, a coreceptor for TLR4, is upregulated by LPS and is essential for Mo-DC differentiation via Trif signaling.

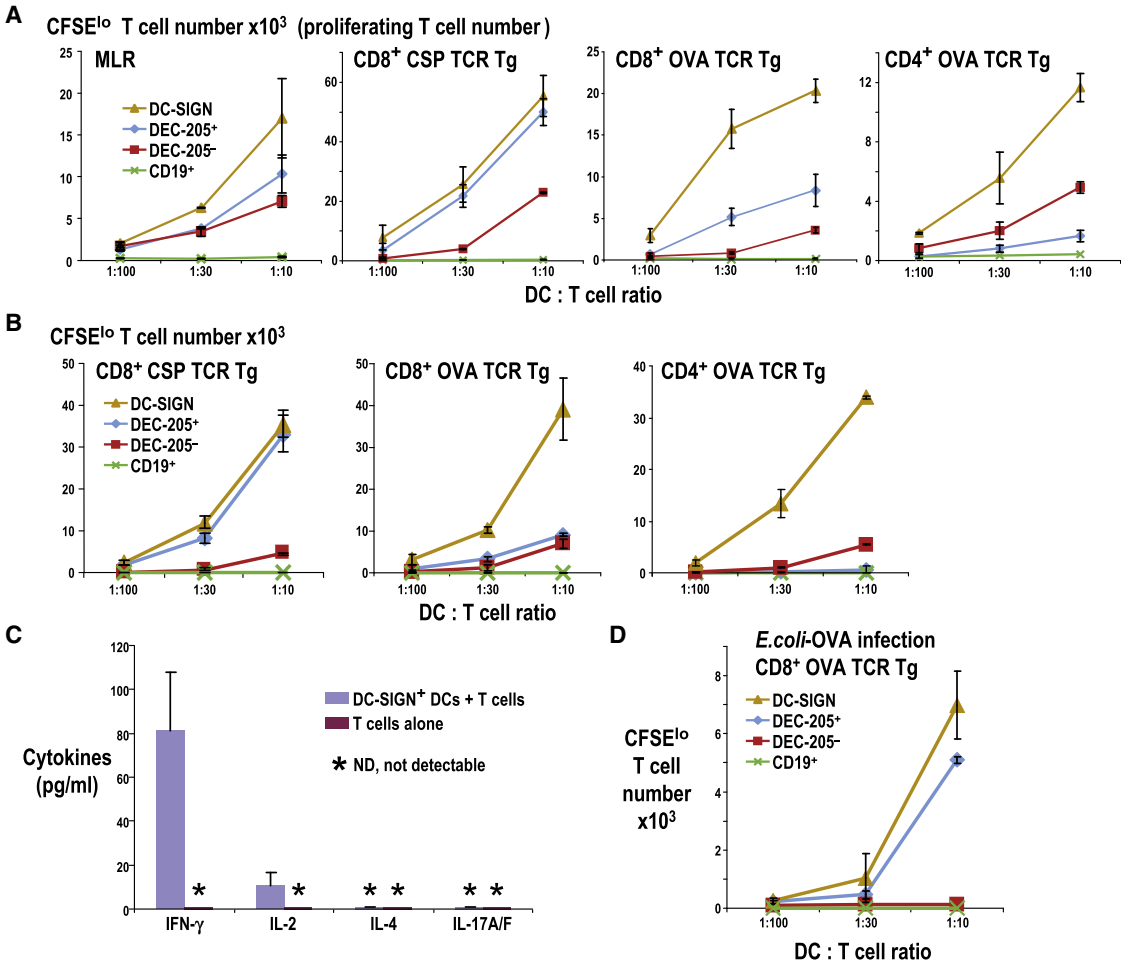

Figure 6. Presentation of Malaria CS and OVA Proteins by Three Types of DCs

(A). C57BL/6 or B6 × BALB/c F1 mice were injected i.v. with 5 μg LPS for 12 hr to isolate three DC fractions (>95% purity), as in Figure 3B. Graded doses were added with 40 μg/ml protein to 50,000 CFSE-labeled T cells, and 3–4 days later, $CFSE^{lo}$ T cells were counted. An MLR was also run to verify DC activity.

(B) As in (A), but mice received 5 μg of LPS i.v. for 12 hr, as well as 50 μg of CSP or OVA protein s.c. in each paw for 2 hr before DC and B cell isolation. Representative data of two experiments in triplicate or quadruplicate cultures are shown. Error bars = SD.

(C) As in (B), but enzyme-linked immunosorbent assay (ELISA) was used to measure the indicated cytokines in the medium of cocultures in which different types of lymph node DCs were used to present OVA to OT-II $CD4^+$ T cells. Error bars = SD.

(D) 5–10 $\times 10^6$ live *E. coli*-OVA or control *E. coli* were injected s.c. with 10 μg MMD3 mAb. Twelve hours later, three populations of lymph node DCs were isolated and used to stimulate OT-I $CD8^+$ T cells. This is representative of two experiments in triplicate. Error bars = SD.

To find out if selective expression of CD14 provided an independent means to isolate Mo-DCs after injecting antigens in vivo, we compared CD14 surface labeling to MMD3 in vivo labeling. With either approach, Mo-DCs were similar and superior cross-presenting DCs (Figure 7E). Thus monocyte differentiation to DCs in response to LPS requires CD14, which serves as an alternative marker to identify and isolate Mo-DCs from classical DCs.

DISCUSSION

One can use the term "authentic" for the Mo-DCs described here for several reasons, which have not previously been noted for inflammatory monocytes. The Mo-DCs are dendritic cells in terms of their motility because they are nonadherent cells that continually form and retract processes in the living state, identical to the probing morphology of DCs in the T cell areas of living LNs (Lindquist et al., 2004). These Mo-DCs also concentrate in the T cell areas, again a classic feature of DCs and a location that facilitates clonal selection of antigen-specific T cells from the recirculating repertoire. The Mo-DCs are very similar in phenotype to DCs in lymphoid tissues including the loss of markers that were used previously to positively identify inflammatory monocytes in vivo, i.e., Ly6C and Gr-1 antigens and CD115/c-fms receptor.

Importantly, when Mo-DCs are compared functionally to classical DCs from the same LNs, the former are not only active but can be superior in stimulating the MLR and in presenting protein antigens, administered in vitro and also in vivo prior to testing as presenting cells. A large amount of previous emphasis has been

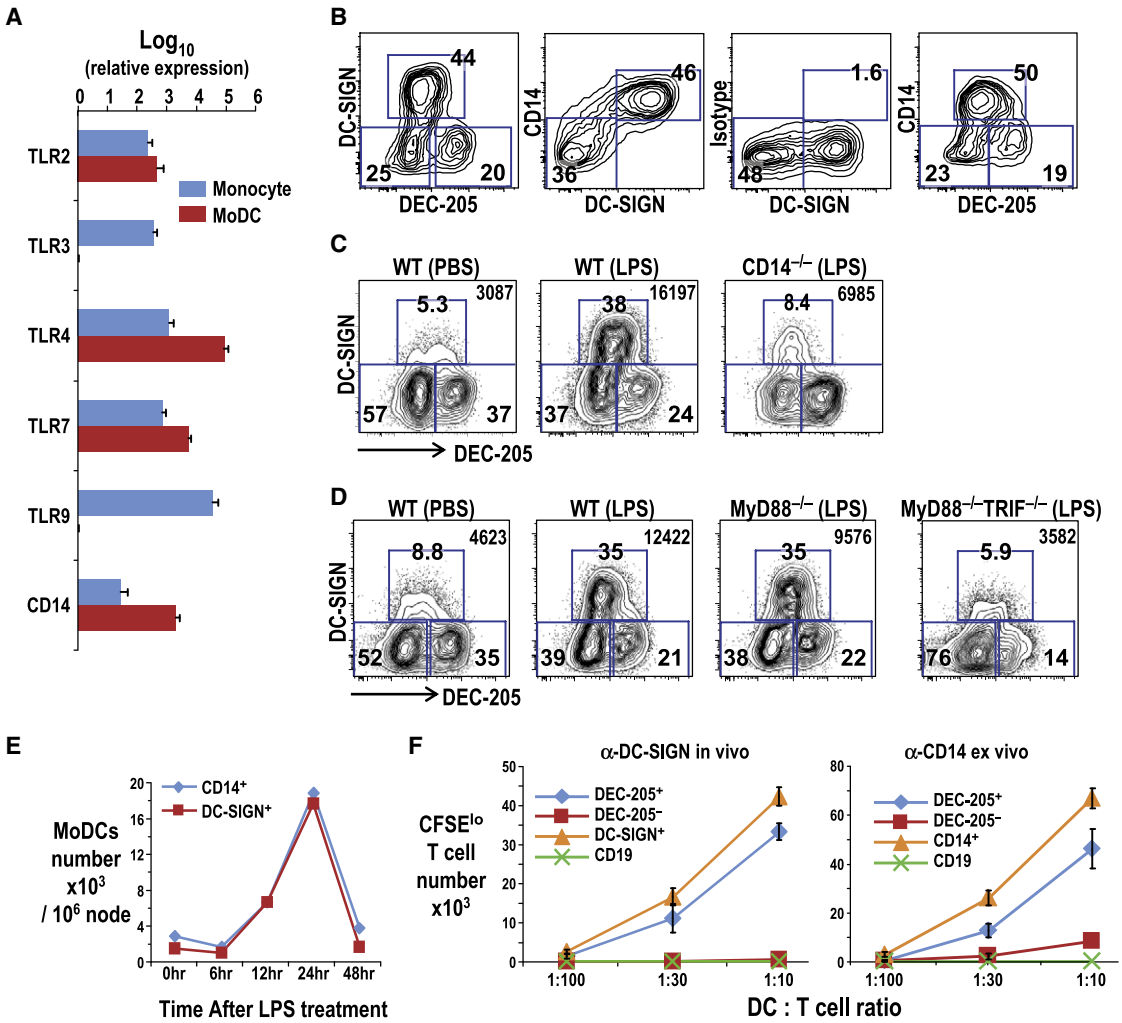

Figure 7. Mo-DCs Selectively Express CD14, a Required Coreceptor for Their Mobilization

(A) Quantitative PCR to assess expression of mRNA for several TLRs and CD14 in marrow monocytes and Mo-DCs. Error bars = SD.

(B) DC-SIGN$^+$ Mo-DCs colabel for CD14 expression.

(C) CD14$^{-/-}$ mice fail to mobilize Mo-DCs in response to LPS.

(D) DC-SIGN$^+$ Mo-DCs are mobilized in MyD88$^{-/-}$ but not MyD88$^{-/-}$ × Trif$^{-/-}$ mice. The numbers of DC-SIGN$^+$ Mo-DCs per million lymph node cells are on the panels.

(E) Kinetics of formation and disappearance of Mo-DCs in LNs from LPS-treated mice, monitored by in vivo labeling of lymphocyte-negative, CD11c^{hi} DCs with MMD3 anti-DC-SIGN mAb or by ex vivo labeling for CD14. Mo-DC's numbers are averages of two mice each per time point.

(F) Mice were injected with LPS for 12 hr, and 2 hr prior to isolation CSP was injected. Mo-DCs were labeled either with MMD3 mAb in vivo or with anti-CD14 ex vivo and used to stimulate CSP-specific CD8$^+$ T cells.

Error Bars = SD. Representative data of at least two independent experiments (A–F) are shown.

placed on the superior cross-presenting activity of the CD8$^+$ or DEC-205$^+$ subset of DCs, but the Mo-DCs we describe can be equally or more effective than CD8$^+$ DCs, including for bacteria injected in vivo. Thus Mo-DCs are equivalent in many functional respects to DCs, except that they are monocyte dependent, whereas numerous prior studies show that classical DCs are monocyte independent (Naik et al., 2006; Varol et al., 2007) and derive from a committed pre-cDC in the bone marrow (Liu et al., 2009). None of these new functional features of Mo-DCs have been described before for monocyte-derived cells in various inflammatory conditions.

The finding that permitted our research was the derivation of mAbs to DC-SIGN or CD209a that recognized this lectin in tissue sections, much of which are intracellular in location (Cheong et al., 2010). The new anti-DC-SIGN/CD209a mAbs allowed us to visualize the LPS-induced mobilization of Mo-DCs in the T cell areas and distinguish them from the resident DCs there. Previously, a combination of CD11b and CD11c markers were used to help identify inflammatory monocytes with some features of DCs (Leon et al., 2007; Serbina et al., 2003; Nakano et al., 2009; Hohl et al., 2009; Siddiqui et al., 2010; Kool et al., 2008), but these integrins are not sufficient to permit localization

in situ, and the Mo-DCs actually have lower levels of CD11c than classical DCs. Previous isolations also used antibodies to Ly6C or Gr-1, but these markers are lost from the Mo-DCs described here.

Although DC-SIGN/CD209a was critical for identifying authentic Mo-DCs in vivo, functions for this lectin need research. We showed, for example, that DC-SIGN$^{-/-}$ monocytes become Mo-DCs (marked by MMR/CD206) in the T cell areas, just like WT monocytes, when the mice are given LPS (Figure S2E). Therefore DC-SIGN seems not to be involved in Mo-DC mobilization and differentiation. Also Mo-DCs cultured from DC-SIGN$^{-/-}$ mice still present antigens to OT-I and OT-II transgenic T cells comparably to WT (not shown). DC-SIGN/CD209 can play pathogenic roles, either in transmitting infectious agents like HIV and CMV in the case of cultured human Mo-DCs (Geijtenbeek et al., 2000a; Halary et al., 2002) or in transducing inhibitory signals as seen when human DC-SIGN/CD209 interacts with mycobacteria (Geijtenbeek et al., 2003; Tailleux et al., 2003). DC-SIGN/CD209 could also have protective functions for capture and presentation of glycan-modified antigens (Tacken et al., 2005). Also the pathway described here to mobilize DC-SIGN/CD209a^{+} DCs could generate new vaccination strategies, given the powerful antigen presentation and immune stimulatory consequences of this full DC differentiation pathway.

We have identified one molecular pathway to produce Mo-DCs in vivo, which is rapid differentiation from blood monocytes upon administration of TLR4 agonists to mice. The classical method to produce DC-SIGN/CD209^{+} MMR/CD206^{+} Mo-DCs from human (Romani et al., 1994; Sallusto and Lanzavecchia, 1994) and mouse (Schreurs et al., 1999; Agger et al., 2000) blood monocytes takes several days of culture in GM-CSF and IL-4, but here we show that LPS and LPS^{+} live and dead bacteria act rapidly within hours. Blood monocytes drop to 20% of their normal levels 6–12 hr after i.v. LPS, and at the same time, cells move into LNs and differentiate into DC-SIGN/CD209a^{+} MMR/CD206^{+} Mo-DCs. This influx requires CCR7 and CD62L, both expressed by bone marrow and blood monocytes. Among the agonists for Toll-like receptors that we studied, only LPS via TLR4 had this capacity to induce Mo-DCs. In spite of hundreds of studies of the response of mice to LPS, this mobilization of antigen-presenting cells was not previously appreciated.

To explain the peculiar role of TLR4 agonists, we first examined gene expression for several TLRs. Whereas monocytes expressed many TLRs, only TLR4 increased markedly when monocytes differentiated into Mo-DCs in culture. This was also the case for the CD14 coreceptor for TLR4, which mediates MyD88-independent and Trif-dependent TLR4 signaling (Jiang et al., 2005). Xu et al. have shown previously that GM-CSF/IL-4-derived DCs produce cytokines in response to several agonists, e.g., Pam3Cys and ODN1826 (Xu et al., 2007), which we found did not mobilize Mo-DCs from monocytes in vivo. However, a key feature of the Mo-DCs that are mobilized by LPS is that they express CD14, which not only proved to be an independent marker for Mo-DCs but was also essential for their generation.

We would like to propose that the mobilization of Mo-DCs described here has two roles. One is part of the innate response to gram-negative bacteria and other agents that contain agonists for the TLR4-CD14 complex, although this will require additional studies of the functional properties of Mo-DCs such as the production of cytokines and chemokines. A second is as a segue to the adaptive immune response. During the TLR4-based response, Mo-DCs increase while classical DCs decrease, so that Mo-DCs become the dominant cell for induction of effective and combined CD4^{+} and CD8^{+} T cell immunity, with or without the requirement for bacterial replication in this newly mobilized DC reservoir.

EXPERIMENTAL PROCEDURES

Mice

DC-SIGN$^{-/-}$ mice were from the Consortium for Functional Glycomics (Scripps Res. Inst., La Jolla, CA, USA). Flt3$^{-/-}$ (I.R. Lemischka, Mount Sinai School of Medicine), GMCSF-R$^{-/-}$ (G. Begley, Amgen), MyD88$^{-/-}$(S. Akira, Univ. of Osaka), and MyD88$^{-/-}$ × Trif$^{-/-}$ (E. Pamer, Memorial Sloan-Kettering Cancer Center) were provided by M. Nussenzweig (Rockefeller Univ.), iDTR mice by A. Waisman (Univ. of Mainz), and FcR $\gamma^{-/-}$ mice by J. Ravetch (Rockefeller Univ.). C57BL/6 (CD45.1 or CD45.2), C3H/HeJ, chemokine receptor (CCR2, CCR5, CCR6, and CCR7), Lysozyme-M Cre (LysMcre), and CD14$^{-/-}$mice were from Jackson Labs and C3H/HeN and splenectomized mice from Taconic Farms. Mice in specific pathogen-free conditions were studied at 6–10 weeks according to institutional guidelines of the Rockefeller University.

Lipopolysaccharide and Bacteria

LPS from *E. coli* 055:B5 (Sigma) was given i.v., s.c., or intraperitoneally (i.p.) at a dose of 5 μg to induce Mo-DCs. For optimal LPS activity, stocks had to be dissolved at 10 μg/μl or higher. Other TLR agonists were purchased from Invivogen and injected i.v. at 5 μg/mouse. We also tested bacteria at a dose of 5 × 10^6 per mouse, both heat-killed and live bacteria (*E. coli* DH5α, *B. subtilis*). To evaluate presentation of proteins from bacteria, recombinant *E. coli* expressing OVA was used.

Bone Marrow Monocytes and DCs

Monocytes were sorted on a FACSAria (BD Biosciences) as SSC^{lo}, CD11b^{hi}, Ly6C^{hi} or as Ly6G^{-}, CD11b^{hi}, Ly6C^{hi} cells, the latter ensuring higher yields. To generate Mo-DCs, monocytes were cultured with cytokines (M-CSF, GM-CSF, GM-CSF, IL-4; PeproTech) at 20 ng/ml or Flt3-L at 200 ng/ml in RPMI with 5% FBS and antibiotic-antimycotic plus β-mercaptoethanol (Invitrogen). At 4–7 days, nonadherent cells were removed to test function, or for M-CSF, adherent cells were recovered with Cellstripper nonenzymatic cell dissociation solution (Mediatech). Alternatively, to generate DCs, total bone marrow was cultured with Flt3-L (400 ng/ml) for 9 days as described (Naik et al., 2005), and the equivalents of CD8^{+} and CD8^{-} spleen DCs were sorted as CD24^{hi} CD11b^{lo} and CD24^{lo} CD11b^{hi} cells, respectively.

Monocyte and Bone Marrow Transfer

2 × 10^6 CD45.2^{+} marrow monocytes were transferred to 4- to 6-week CD45.1^{+} mice (>8 weeks gave poor results). For mixed marrow chimeras, 50:50 mixtures of knockout (KO) and WT marrow were injected i.v. into lethally irradiated (5.5 Gy twice, 3 hr apart) mice. To deplete monocytes, DT (Sigma) in PBS (1 μg/μl, stored at −80°C) was injected i.v. to LysMcre × iDTR mice at 25 ng/g weight (~500 ng/mouse).

Antibodies, Flow Cytometry, and Microscopy

Rabbit polyclonal antibody to a 14 amino acid cytoplasmic domain peptide of DC-SIGN and mAbs to DC-SIGN (BMD10, BMD30, and MMD3) were described (Cheong et al., 2010). mAbs were conjugated with biotin or Alexa 647 (Invitrogen) following manufacturer's instructions. These bound specifically to CHO cells stably expressing mouse DC-SIGN. 22D1 (α-SIGN-R1/CD209b), SER4 (α-CD169), L31 (α-CD207), NLDC145 (α-DEC-205/CD205), N418 (α-CD11c), KL295 (α-MHC II I-A$^{b/d}$ β), GL117 (rat IgG2a

control), and MEL-14 (α-CD62L) mAbs were purified from hybridoma supernatants or purchased from eBioscience, and they were tested to be endotoxin free (QCL-1000 kit, BioWhittaker). We purchased mAbs conjugated to different fluorochromes to CD19, CD3, NK1.1, DX-5, CD206, CD11b, I-A/I-E (MHC II), CD135, CD172a, CD14, and Ly6G from BD Bioscience; MMR/CD206 from Biolegend; PE-α-mouse CD115, CD8α, Gr-1, CD11b, CD40, CD24, Mac-3, CD62L, and CD14 from eBioscience; F4/80 and Ly6C (PE or Alexa 647) from AbD Serotec. For BrdU labeling, 200 μl of 10 mg/ml of BrdU was injected i.p. for 12 hr; staining followed manufacturer's instruction (FITC BrdU flow kit, BD).

Lymph Node Cells and Sections

Skin-draining nodes were treated with collagenase D (400 U/ml) for 30 min at 37°C. Cells were preincubated 10 min with 2.4G2 mAb at 4°C to block Fc receptors, stained with fluorescent mAbs, acquired on a BD-LSRII, and analyzed using flowjo (Treestar). To label Mo-DCs in vivo, we injected 10 μg of Alexa 647-MMD3 α-DC-SIGN or control mouse IgG2c mAb along with LPS. Lymphocytes ($CD3^+$, $CD19^+$, $DX5^+$, or $NK1\text{-}1^+$) and $B220^+$ plasmacytoid DCs were excluded, and three populations of $CD11c^{hi}$ cells were separated as DC-$SIGN^+$, DEC-205^+ (Alexa 488-NLDC145 mAb) and DEC-205^- DC-$SIGN^-$ DCs. $CD19^+$ cells were also sorted. 10 μm OCT-embedded lymph node sections were acetone-fixed, stained with BMD10 or BMD30 CD209a mAb for 1 hr at room temperature or 4°C overnight, followed by mouse anti-rat IgG2a-HRP for 30 min and Tyramide-signal amplification (Invitrogen). B220-Alexa 647 stained B cell areas in confocal microscopy (LSM510, Zeiss). We also injected into live mice 30 μg Alexa 488 MMD3 anti-DC-SIGN or isotype control mAb i.v. Tissues were fixed in 4% HCHO/PBS for 20 min, then 0.5% Triton X-100 for 15 min, and stained with rabbit anti-Alexa 488 and anti-rabbit HRP to label using TSA Alexa 488. For live-cell DIC imaging, Mo-DCs were seeded on glass bottom culture dishes (MatTek) and examined in an Olympus LCV110U incubator fluorescence microscope. Confocal and live-cell images were analyzed with MetaMorph software (Universal Imaging).

Splenic Monocytes and DCs

These were sorted from collagenase-digested spleen as monocytes ($CD19^-$ $CD3^-$ $DX\text{-}5^-$ $CD11b^+$ $CD11c^{dim}$ $Ly6G^-$ $Ly6C^+$) and two classical DC subsets ($CD19^-$ $CD3^-$ $DX\text{-}5^-$ $CD11c^{hi}$ and either DEC-205^+ or DEC-205^- cells).

Antigen Presentation

T cells specific for OVA (OT-I, OT-II) or malarial (*P. yoeli*) circumsporozoite protein (CSP) were cultured with graded doses of DCs or B cells. OVA (LPS-free, Seikagaku Corp.) or CSP (Choi et al., 2009) was added in graded doses but usually at 40 μg/ml in vitro, or the proteins were injected for 2 hr in vivo (50 μg/foot pad) during LPS mobilization of Mo-DCs. In some experiments, we used irradiated CHO cells stably transduced with OVA as the source of antigen. Splenic transgenic T cells were enriched after Fc block by excluding $B220^+$, $F4/80^+$, $NK1.1^+$, $I\text{-}Ab^+$, and $CD4^+$ or $CD8^+$ T cells using anti-rat IgG Dynabeads (Invitrogen), labeled with 5 μM CFSE (Invitrogen) and added to round bottom microtest wells at 50,000/well. After 3 days for OT-I or 4 days for OT-II and CS T cells, proliferation of live (Aqua dye negative, Invitrogen) T cells was evaluated by CFSE dilution and staining with mAb to Vα2 for the OT-I or OT-II TCR and Vβ8.1/8.2 for CSP. For the MLR, DCs from C57BL/6 mice were added in graded doses to CFSE-labeled BALB/c T cells (NK1.1, I-A, B220, F4/80 negative cells) and assayed at day 4.

Quantitative PCR for TLR and CD14 Expression by Monocytes and Mo-DCs

Taqman probes (AssayID) were used for TLR4 (Mm00445273_m1), TLR2 (Mm00442346_m1), TLR3 (Mm00628112_m1), TLR7(Mm00446590_m1), TLR9 (Mm00446193_m1), and CD14(Mm00438094_g1) from Applied Biosystems. The relative expression was normalized by TATA-box binding protein (TBP) housekeeping gene expression. All qPCR experiments were performed with LightCycler 480 Real-Time PCR System (Roche).

SUPPLEMENTAL INFORMATION

Supplemental Information includes seven figures and one movie and can be found with this article online at doi:10.1016/j.cell.2010.09.039.

ACKNOWLEDGMENTS

We thank members of the Steinman lab for valuable discussion, J. Adams for graphics, A.J. North and S.A. Galdeen for DIC imaging at the bioimaging resource center, S. Mazel and C. Bare for flow cytometry at the resource center of Rockefeller University, Y. Oh and I. Jang for CSP preparation, J.D. Schauer for mAb purification, J. Gonzalez for ELISA assays (Rockefeller University Center for Clinical and Translational Science, UL1RR024143 from National Center for Research Resource). We thank the Consortium for Functional Glycomics supported by NIGMS (GM62116) for DC-SIGN/CD209a$^{-/-}$ mice. We were supported by grants from the NIH (AI40045 and AI40874), the Bill and Melinda Gates Foundation (R.M.S.), New York Community Trust's Francis Florio funds for blood diseases (C.C.), and a Fundação para a Ciência e Tecnologia PhD scholarship (I.M. SFRH/BD/41073/2007).

Received: May 11, 2010
Revised: August 10, 2010
Accepted: September 23, 2010
Published: October 28, 2010

REFERENCES

Agger, R., Petersen, M.S., Toldbod, H.E., Holtz, S., Dagnaes-Hansen, F., Johnsen, B.W., Bolund, L., and Hokland, M. (2000). Characterization of murine dendritic cells derived from adherent blood mononuclear cells in vitro. Scand. J. Immunol. *52*, 138–147.

Cheong, C., Matos, I., Choi, J.H., Schauer, J.D., Dandamudi, D.B., Shrestha, E., Makeyeva, J.A., Li, X., Li, P., Steinman, R.M., et al. (2010). New monoclonal anti-mouse DC-SIGN antibodies reactive with acetone-fixed cells. J. Immunol. Methods *360*, 66–75.

Choi, J.H., Do, Y., Cheong, C., Koh, H., Boscardin, S.B., Oh, Y.S., Bozzacco, L., Trumpfheller, C., Park, C.G., and Steinman, R.M. (2009). Identification of antigen-presenting dendritic cells in mouse aorta and cardiac valves. J. Exp. Med. *206*, 497–505.

D'Amico, A., and Wu, L. (2003). The early progenitors of mouse dendritic cells and plasmacytoid predendritic cells are within the bone marrow hemopoietic precursors expressing Flt3. J. Exp. Med. *198*, 293–303.

de Villiers, W.J.S., Fraser, I.P., Hughes, D.A., Doyle, A.G., and Gordon, S. (1994). Macrophage-colony-stimulating factor selectively enhances macrophage scavenger receptor expression and function. J. Exp. Med. *180*, 705–709.

De Vries, I.J., Krooshoop, D.J., Scharenborg, N.M., Lesterhuis, W.J., Diepstra, J.H., Van Muijen, G.N., Strijk, S.P., Ruers, T.J., Boerman, O.C., Oyen, W.J., et al. (2003). Effective migration of antigen-pulsed dendritic cells to lymph nodes in melanoma patients is determined by their maturation state. Cancer Res. *63*, 12–17.

den Haan, J.M., Lehar, S.M., and Bevan, M.J. (2000). $CD8^+$ but not $CD8^-$ dendritic cells cross-prime cytotoxic T cells in vivo. J. Exp. Med. *192*, 1685–1696.

Dhodapkar, M., Steinman, R.M., Sapp, M., Desai, H., Fossella, C., Krasovsky, J., Donahoe, S.M., Dunbar, P.R., Cerundolo, V., Nixon, D.F., et al. (1999). Rapid generation of broad T-cell immunity in humans after single injection of mature dendritic cells. J. Clin. Invest. *104*, 173–180.

Dudziak, D., Kamphorst, A.O., Heidkamp, G.F., Buchholz, V., Trumpfheller, C., Yamazaki, S., Cheong, C., Liu, K., Lee, H.W., Park, C.G., et al. (2007). Differential antigen processing by dendritic cell subsets *in vivo*. Science *315*, 107–111.

Fogg, D.K., Sibon, C., Miled, C., Jung, S., Aucouturier, P., Littman, D.R., Cumano, A., and Geissmann, F. (2006). A clonogenic bone marrow progenitor specific for macrophages and dendritic cells. Science *311*, 83–87.

Geijtenbeek, T.B.H., Kwon, D.S., Torensma, R., van Vliet, S.J., van Duijnhoven, G.C.F., Middel, J., Cornelissen, I.L.M.H.A., Nottet, H.S.L.M., KewalRamani, V.N., Littman, D.R., et al. (2000a). DC-SIGN, a dendritic cell specific HIV-1 binding protein that enhances *trans*-infection of T cells. Cell *100*, 587–597.

Geijtenbeek, T.B.H., Torensma, R., van Vliet, S.J., van Duijnhoven, G.C.F., Adema, G.J., van Kooyk, Y., and Figdor, C.G. (2000b). Identification of DC-SIGN, a novel dendritic cell-specific ICAM-3 receptor that supports primary immune responses. Cell *100*, 575–585.

Geijtenbeek, T.B., van Vliet, S.J., Koppel, E.A., Sanchez-Hernandez, M., Vandenbroucke-Grauls, C.M., Appelmelk, B., and van Kooyk, Y. (2003). Mycobacteria target DC-SIGN to suppress dendritic cell function. J. Exp. Med. *197*, 7–17.

Geissmann, F., Jung, S., and Littman, D.R. (2003). Blood monocytes consist of two principal subsets with distinct migratory properties. Immunity *19*, 71–82.

Geissmann, F., Manz, M.G., Jung, S., Sieweke, M.H., Merad, M., and Ley, K. (2010). Development of monocytes, macrophages, and dendritic cells. Science *327*, 656–661.

Ginhoux, F., Tacke, F., Angeli, V., Bogunovic, M., Loubeau, M., Dai, X.M., Stanley, E.R., Randolph, G.J., and Merad, M. (2006). Langerhans cells arise from monocytes in vivo. Nat. Immunol. *7*, 265–273.

Ginhoux, F., Liu, K., Helft, J., Bogunovic, M., Greter, M., Hashimoto, D., Price, J., Yin, N., Bromberg, J., Lira, S.A., et al. (2009). The origin and development of nonlymphoid tissue $CD103^+$ DCs. J. Exp. Med. *206*, 3115–3130.

Goren, I., Allmann, N., Yogev, N., Schurmann, C., Linke, A., Holdener, M., Waisman, A., Pfeilschifter, J., and Frank, S. (2009). A transgenic mouse model of inducible macrophage depletion: effects of diphtheria toxin-driven lysozyme M-specific cell lineage ablation on wound inflammatory, angiogenic, and contractive processes. Am. J. Pathol. *175*, 132–147.

Granelli-Piperno, A., Pritsker, A., Pack, M., Shimeliovich, I., Arrighi, J.-F., Park, C.G., Trumpfheller, C., Piguet, V., Moran, T.M., and Steinman, R.M. (2005). Dendritic cell-specific intercellular adhesion molecule 3-grabbing nonintegrin/CD209 is abundant on macrophages in the normal human lymph node and is not required for dendritic cell stimulation of the mixed leukocyte reaction. J. Immunol. *175*, 4265–4273.

Halary, F., Amara, A., Lortat-Jacob, H., Messerle, M., Delaunay, T., Houles, C., Fieschi, F., Arenzana-Seisdedos, F., Moreau, J.F., and Dechanet-Merville, J. (2002). Human cytomegalovirus binding to DC-SIGN is required for dendritic cell infection and target cell trans-infection. Immunity *17*, 653–664.

Heard, J.M., Roussel, M.F., Rettenmier, C.W., and Sherr, C.J. (1987). Multilineage hematopoietic disorders induced by transplantation of bone marrow cells expressing the v-fms oncogene. Cell *51*, 663–673.

Heath, W.R., and Carbone, F.R. (2001). Cross-presentation, dendritic cells, tolerance and immunity. Annu. Rev. Immunol. *19*, 47–64.

Heath, W.R., and Carbone, F.R. (2009). Dendritic cell subsets in primary and secondary T cell responses at body surfaces. Nat. Immunol. *10*, 1237–1244.

Hohl, T.M., Rivera, A., Lipuma, L., Gallegos, A., Shi, C., Mack, M., and Pamer, E.G. (2009). Inflammatory monocytes facilitate adaptive CD4 T cell responses during respiratory fungal infection. Cell Host Microbe *6*, 470–481.

Jiang, Z., Georgel, P., Du, X., Shamel, L., Sovath, S., Mudd, S., Huber, M., Kalis, C., Keck, S., Galanos, C., et al. (2005). CD14 is required for MyD88-independent LPS signaling. Nat. Immunol. *6*, 565–570.

Johnson, W.D., Jr., Mei, B., and Cohn, Z.A. (1977). The separation, long-term cultivation, and maturation of the human monocyte. J. Exp. Med. *146*, 1613–1626.

Kool, M., Soullie, T., van Nimwegen, M., Willart, M.A., Muskens, F., Jung, S., Hoogsteden, H.C., Hammad, H., and Lambrecht, B.N. (2008). Alum adjuvant boosts adaptive immunity by inducing uric acid and activating inflammatory dendritic cells. J. Exp. Med. *205*, 869–882.

Leon, B., Lopez-Bravo, M., and Ardavin, C. (2007). Monocyte-derived dendritic cells formed at the infection site control the induction of protective T helper 1 responses against *Leishmania*. Immunity *26*, 519–531.

Lindquist, R.L., Shakhar, G., Dudziak, D., Wardemann, H., Eisenreich, T., Dustin, M.L., and Nussenzweig, M.C. (2004). Visualizing dendritic cell networks *in vivo*. Nat. Immunol. *5*, 1243–1250.

Liu, K., Iyoda, T., Saternus, M., Kimura, Y., Inaba, K., and Steinman, R.M. (2002). Immune tolerance after delivery of dying cells to dendritic cells in situ. J. Exp. Med. *196*, 1091–1097.

Liu, K., Victora, G.D., Schwickert, T.A., Guermonprez, P., Meredith, M.M., Yao, K., Chu, F.F., Randolph, G.J., Rudensky, A.Y., and Nussenzweig, M.C. (2009). In vivo analysis of dendritic cell development and homeostasis. Science *324*, 392–397.

Luckashenak, N., Schroeder, S., Endt, K., Schmidt, D., Mahnke, K., Bachmann, M.F., Marconi, P., Deeg, C.A., and Brocker, T. (2008). Constitutive crosspresentation of tissue antigens by dendritic cells controls $CD8^+$ T cell tolerance in vivo. Immunity *28*, 521–532.

Melief, C.J. (2008). Cancer immunotherapy by dendritic cells. Immunity *29*, 372–383.

Mempel, T.R., Henrickson, S.E., and Von Andrian, U.H. (2004). T-cell priming by dendritic cells in lymph nodes occurs in three distinct phases. Nature *427*, 154–159.

Miller, M.J., Safrina, O., Parker, I., and Cahalan, M.D. (2004). Imaging the single cell dynamics of $CD4^+$ T cell activation by dendritic cells in lymph nodes. J. Exp. Med. *200*, 847–856.

Moron, V.G., Rueda, P., Sedlik, C., and Leclerc, C. (2003). In vivo, dendritic cells can cross-present virus-like particles using an endosome-to-cytosol pathway. J. Immunol. *171*, 2242–2250.

Naik, S.H., Proietto, A.I., Wilson, N.S., Dakic, A., Schnorrer, P., Fuchsberger, M., Lahoud, M.H., O'Keeffe, M., Shao, Q.X., Chen, W.F., et al. (2005). Generation of splenic $CD8^+$ and $CD8^-$ dendritic cell equivalents in Fms-like tyrosine kinase 3 ligand bone marrow cultures. J. Immunol. *174*, 6592–6597.

Naik, S.H., Metcalf, D., van Nieuwenhuijze, A., Wicks, I., Wu, L., O'Keeffe, M., and Shortman, K. (2006). Intrasplenic steady-state dendritic cell precursors that are distinct from monocytes. Nat. Immunol. *7*, 663–671.

Naik, S.H., Sathe, P., Park, H.Y., Metcalf, D., Proietto, A.I., Dakic, A., Carotta, S., O'Keeffe, M., Bahlo, M., Papenfuss, A., et al. (2007). Development of plasmacytoid and conventional dendritic cell subtypes from single precursor cells derived *in vitro* and *in vivo*. Nat. Immunol. *8*, 1217–1226.

Nakano, H., Lin, K.L., Yanagita, M., Charbonneau, C., Cook, D.N., Kakiuchi, T., and Gunn, M.D. (2009). Blood-derived inflammatory dendritic cells in lymph nodes stimulate acute T helper type 1 immune responses. Nat. Immunol. *10*, 394–402.

Onai, N., Obata-Onai, A., Schmid, M.A., Ohteki, T., Jarrossay, D., and Manz, M.G. (2007). Identification of clonogenic common $Flt3^+M\text{-}CSFR^+$ plasmacytoid and conventional dendritic cell progenitors in mouse bone marrow. J. Exp. Med. *193*, 233–238.

Park, C.G., Takahara, K., Umemoto, E., Yashima, Y., Matsubara, K., Matsuda, Y., Clausen, B.E., Inaba, K., and Steinman, R.M. (2001). Five mouse homologues of the human dendritic cell C-type lectin, DC-SIGN. Int. Immunol. *13*, 1283–1290.

Regnault, A., Lankar, D., Lacabanne, V., Rodriguez, A., Thery, C., Rescigno, M., Saito, T., Verbeek, S., Bonnerot, C., Ricciardi-Castagnoli, P., et al. (1999). Fcγ receptor-mediated induction of dendritic cell maturation and major histocompatibility complex class I-restricted antigen presentation after immune complex internalization. J. Exp. Med. *189*, 371–380.

Romani, N., Gruner, S., Brang, D., Kämpgen, E., Lenz, A., Trockenbacher, B., Konwalinka, G., Fritsch, P.O., Steinman, R.M., and Schuler, G. (1994). Proliferating dendritic cell progenitors in human blood. J. Exp. Med. *180*, 83–93.

Sallusto, F., and Lanzavecchia, A. (1994). Efficient presentation of soluble antigen by cultured human dendritic cells is maintained by granulocyte/macrophage colony-stimulating factor plus interleukin 4 and downregulated by tumor necrosis factor α. J. Exp. Med. *179*, 1109–1118.

Sallusto, F., Cella, M., Danieli, C., and Lanzavecchia, A. (1995). Dendritic cells use macropinocytosis and the mannose receptor to concentrate

macromolecules in the major histocompatibility class II compartment: down-regulation by cytokines and bacterial products. J. Exp. Med. *182*, 389–400.

Sancho, D., Joffre, O.P., Keller, A.M., Rogers, N.C., Martinez, D., Hernanz-Falcon, P., Rosewell, I., and Reis e Sousa, C. (2009). Identification of a dendritic cell receptor that couples sensing of necrosis to immunity. Nature *458*, 899–903.

Schnorrer, P., Behrens, G.M., Wilson, N.S., Pooley, J.L., Smith, C.M., El-Sukkari, D., Davey, G., Kupresanin, F., Li, M., Maraskovsky, E., et al. (2006). The dominant role of $CD8^+$ dendritic cells in cross-presentation is not dictated by antigen capture. Proc. Natl. Acad. Sci. USA *103*, 10729–10734.

Schreurs, M.W.J., Eggert, A.A.O., de Boer, A.J., Figdor, C.G., and Adema, G.J. (1999). Generation and functional characterization of mouse monocyte-derived dendritic cells. Eur. J. Immunol. *29*, 2835–2841.

Schuler-Thurner, B., Dieckmann, D., Keikavoussi, P., Bender, A., Maczek, C., Jonuleit, H., Roder, C., Haendle, I., Leisgang, W., Dunbar, R., et al. (2000). Mage-3 and influenza-matrix peptide-specific cytotoxic T cells are inducible in terminal stage HLA-A.2.1^+ melanoma patients by mature monocyte-derived dendritic cells. J. Immunol. *165*, 3492–3496.

Serbina, N.V., Salazar-Mather, T.P., Biron, C.A., Kuziel, W.A., and Pamer, E.G. (2003). TNF/iNOS-producing dendritic cells mediate innate immune defense against bacterial infection. Immunity *19*, 59–70.

Shakhar, G., Lindquist, R.L., Skokos, D., Dudziak, D., Huang, J.H., Nussenzweig, M.C., and Dustin, M.L. (2005). Stable T cell-dendritic cell interactions precede the development of both tolerance and immunity *in vivo*. Nat. Immunol. *6*, 707–714.

Siddiqui, K.R., Laffont, S., and Powrie, F. (2010). E-cadherin marks a subset of inflammatory dendritic cells that promote T cell-mediated colitis. Immunity *32*, 557–567.

Steinman, R.M., and Cohn, Z.A. (1973). Identification of a novel cell type in peripheral lymphoid organs of mice. I. Morphology, quantitation, tissue distribution. J. Exp. Med. *137*, 1142–1162.

Steinman, R.M., and Witmer, M.D. (1978). Lymphoid dendritic cells are potent stimulators of the primary mixed leukocyte reaction in mice. Proc. Natl. Acad. Sci. USA *75*, 5132–5136.

Stoll, S., Delon, J., Brotz, T.M., and Germain, R.N. (2002). Dynamic imaging of T cell-dendritic cell interactions in lymph nodes. Science *296*, 1873–1876.

Swirski, F.K., Nahrendorf, M., Etzrodt, M., Wildgruber, M., Cortez-Retamozo, V., Panizzi, P., Figueiredo, J.L., Kohler, R.H., Chudnovskiy, A., Waterman, P., et al. (2009). Identification of splenic reservoir monocytes and their deployment to inflammatory sites. Science *325*, 612–616.

Tacken, P.J., de Vries, I.J., Gijzen, K., Joosten, B., Wu, D., Rother, R.P., Faas, S.J., Punt, C.J., Torensma, R., Adema, G.J., et al. (2005). Effective induction of naive and recall T-cell responses by targeting antigen to human dendritic cells via a humanized anti-DC-SIGN antibody. Blood *106*, 1278–1285.

Tailleux, L., Schwartz, O., Herrmann, J.-L., Pivert, E., Jackson, M., Amara, A., Legres, L., Dreher, D., Nicod, L.P., Gluckman, C.J., et al. (2003). DC-SIGN is the major *Mycobacterium tuberculosis* receptor on human dendritic cells. J. Exp. Med. *197*, 121–127.

Varol, C., Landsman, L., Fogg, D.K., Greenshtein, L., Gildor, B., Margalit, R., Kalchenko, V., Geissmann, F., and Jung, S. (2007). Monocytes give rise to mucosal, but not splenic, conventional dendritic cells. J. Exp. Med. *204*, 171–180.

Vremec, D., and Shortman, K. (1997). Dendritic cells subtypes in mouse lymphoid organs. Cross-correlation of surface markers, changes with incubation, and differences among thymus, spleen, and lymph nodes. J. Immunol. *159*, 565–573.

Waskow, C., Liu, K., Darrasse-Jeze, G., Guermonprez, P., Ginhoux, F., Merad, M., Shengelia, T., Yao, K., and Nussenzweig, M. (2008). The receptor tyrosine kinase Flt3 is required for dendritic cell development in peripheral lymphoid tissues. Nat. Immunol. *9*, 676–683.

Xu, Y., Zhan, Y., Lew, A.M., Naik, S.H., and Kershaw, M.H. (2007). Differential development of murine dendritic cells by GM-CSF versus Flt3 ligand has implications for inflammation and trafficking. J. Immunol. *179*, 7577–7584.